Electronic Supplementary Material (ESI) for Chemical Communications.

Exploiting Le Chatelier's principle for a one-pot synthesis of nontoxic HHogGNPs with the sharpest nanoscopic features suitable for tunable plasmon spectroscopy and high throughput SERS sensing

M. Bhattacharya[a], V. Mazov[b], B. Satpati[c], P. Jena[d], S. Das Chakraborty[a], S. Kumar[e], B. Pathak[e], D. V. Kuznetsov[b] and D. Senapati[a]*

[a]Chemical Sciences Division, Saha Institute of Nuclear Physics, HBNI, 1/AF, Bidhannagar, Kolkata-700064, India

[b]Department of Functional Nanosystems and High Temperature Materials, National University of Science and Technology "MISiS", 4 Leninsky Ave., Moscow 119049, Russia

[c]Surface Physics and Material Science Division, Saha Institute of Nuclear Physics, HBNI, 1/AF, Bidhannagar, Kolkata-700064, India

[d]CRNN, University of Calcutta, JD-2, Salt Lake City, Kolkata-700098, India

[e]Discipline of Chemistry, Discipline of Metallurgy Engineering and Materials Science, IIT Indore, Indore-453552, India

*dulal.senapati@saha.ac.in

1. EXPERIMENTAL SECTION

1.1 Chemicals and Reagents

Chemicals including silver nitrate ($AgNO_3$, BioXtra, >99%, titration), gold(III) chloride trihydrate ($HAuCl_4.3H_2O$, ≥99.9%, impurity metal basis), sodium citrate tribasic dihydrate ($HOC(COONa)(CH_2COONa)_2.2H_2O$, ≥99%), L-ascorbic acid ($C_6H_8O_6$, 99%), hydrochloric acid (HCl, ACS reagent, 37%), sodium hydroxide (NaOH, BioXtra, ≥98%), sodium chloride (NaCl, AR, ≥99.9%) and Rhodamine 6G ($C_{28}H_{31}N_2O_3Cl$, Dye content 99%) were purchased from Sigma-Aldrich and used without further purification. All experiments were performed with Milli-Q water.

1.2 Synthesis of HHogGNPs

As a synthetic protocol, 49mL Milli-Q water was taken in a conical flask to which we added variable amount (0-2500µL) of 1% TSC, 1.25mL of 10mM $HAuCl_4.3H_2O$ solution, 500µL of 1.5mM $AgNO_3$ and 250µL of 10^{-1}M ascorbic acid solution (drop wise) in the mentioned sequence with continuous stirring (300rpm) at room temperature (~25°C). This protocol gives

different TSC based nanostars. For variable amount $AgNO_3$-based nanostars we took fixed amount (750µL) of 1% TSC and the same reaction was carried out with variable amount (200-2500µL) of 1.5mM $AgNO_3$. We prepared different pH solutions in the range of 1-12 either by adding controlled volume of HCl (for pH 1-4) or NaOH (for pH 5-12) in the mother solution. Keeping the molar ratios of TSC, $HAuCl_4.3H_2O$, $AgNO_3$ and ascorbic acid constant (750µL of 1% TSC mixed with 1.25mL of 10^{-2}M $HAuCl_4.3H_2O$, 500µL of 1.5mM $AgNO_3$ and 250µL of 10^{-1}M ascorbic acid) we have generated highly anisotropic hedgehog gold nanoparticles (HHogGNPs) at different lower pH (pH 1-4). Considering the role of HCl by decreasing the solubility of AgCl through 'common ion' effect, we have implemented NaCl (the salt also generates additional chloride ions, Cl^-, in the mother solution to offer same 'common ion' effect as we have discussed for HCl) as a replacement of HCl to form HHogGNPs by keeping pH of the reaction mixture close to neutral. We took 0-1200µL of 1.7M NaCl solution to vary the Cl^- concentration between 250µM to 40.25mM ($HAuCl_4$ solution is the source of 250µM Cl^- in the reaction mixture in absence of NaCl) into 49mL water and added 750µL of 1% TSC, 1.25mL of 10^{-2}M $HAuCl_4.3H_2O$, 500µL of 1.5mM $AgNO_3$ and 250µL of 10^{-1}M ascorbic acid in sequence with continuous stirring at 300rpm at room temperature as mentioned above. In this case, hedgehog nanostructures are obtained particularly when NaCl concentration in the mother solution is 170µM or higher.

After the synthesis of shape tunable HHogGNPs, aliquots were taken from the solutions to centrifuge at 2000-4000rpm for 2h depending on particle's size to remove unbound reagents. These concentrated samples were used for making TEM grids and for carrying out further SERS and toxicity experiments. The detailed synthesis of seed-free, template-free gold nanostar and HHog gold nanoparticles is summarized in **Scheme 1**.

The synthesis with ascorbic acid only (in the absence of TSC, $AgNO_3$ and NaCl) as a control has also been attempted. 1mL of 10^{-2}M ice-cooled $HAuCl_4.3H_2O$ solution was rapidly added into 20mL of ice-cooled solution of 10^{-1}M ascorbic acid with constant stirring (300rpm); the mixture was then kept on ice. A deep blue colour appeared and the corresponding absorption spectra and TEM image has been shown in **Figure S1**. The solution remained stable for months if we kept them in refrigerator.

1.3 Transmission electron microscopy (TEM)

For both the normal and high resolution transmission electron microscopy (HRTEM) measurements we used a FEI, Tecnai G^2F30, S-Twin microscope operating at 120 and 300kV, respectively. Compositional analysis was performed by energy dispersive X-ray spectroscopy (EDS, EDAX Inc.) attached to Tecnai F30. We used simple but modified techniques for close-to-clean monolayer sample preparation both for TEM and SEM. For the TEM measurements we used a 300-mesh copper formvar/carbon grid and followed drop casting as well as a previously described dip-and-dry technique to make the sample where the TEM grid was immersed in the concentrated nanomaterial solution by using a tweezer. Hydrophobic formvar/carbon coating allows building up a monolayer sample stuck to copper mesh dried on a soft tissue paper. After complete drying, the grid was used for TEM measurements.

1.4 Scanning electron microscopy (SEM)

The ZEISS SUPRA 40 scanning electron microscope fitted with a hot Schottky field emission gun (FEG) was used to obtain secondary electron images of the HHogGNPs. For SEM measurements we used pieces of mirror polished silicon wafers as sample support. We injected about 30μL of the concentrated HHog nanomaterial sample on the tilted silicon wafer and the hydrophobicity of the wafer allows only a monolayer of the sample to sticks to the surface which quickly dries to allow an immediate SEM measurement.

1.5 UV-Vis absorption spectroscopy

The UV-visible and vis-NIR absorption spectra were recorded at room temperature on a Jasco V-650 and Jasco V-770 spectrophotometers respectively by using 1 cm quartz cuvette.

1.6 Surface enhanced Raman spectroscopy (SERS)

<u>Instrumental details:</u>

SERS experiments were performed by using a homemade Raman setup and a Thermo Scientific™ DXR™2 commercial Raman microscope for visible and NIR excitation light source respectively. For our home made setup we used a continuous wavelength diode-pumped solid state (DPSS) laser from Laserglow Technologies, Canada (LRS-0671-PFM-00300-03) operating at 671nm as an excitation light source (at fixed excitation energy at 3mW, attenuated by neutral density filter). For focusing and filtering we used an InPhotonics made 670nm fiber optics Raman probe with spectral range 200-3900cm^{-1} (Stokes) for sample excitation and data collection. The Raman probe consists of two single fibers (105µm excitation fiber, 200µm collection fiber) with filtering and steering micro-optics, N.A. 0.22. Excitation fiber was connected to a fiber port to align the laser whereas the collection fiber was connected to the spectrometer. A miniaturized QE65000 scientific grade spectrometer (Ocean Optics) was used as Raman detector with spectral response range 220–3600cm^{-1}. Raman spectrometer is equipped with TE cooled 2048 pixel CCD and interfaced to a computer through a USB port. The Raman spectrum was collected using Ocean Optics data acquisition SpectraSuite spectroscopy software.

For Thermo Scientific™ DXR™2 commercial Raman microscope we used 780nm laser line as the excitation light source with spectral range 3500-50 cm^{-1} (Stokes) for a single exposure of the CCD. Microscope optics is research-quality Olympus viewing optics.

Experimental details:

For carrying out SERS experiments we centrifuged the HHogGNP samples with absorption maxima beyond 600nm at 2000rpm for 2h whereas the samples having absorption maxima below 600nm were centrifuged at 4000rpm for 2h. The lower part thus obtained (~100µL concentrated sample from ~50mL reaction mixture) was collected for executing SERS experiments where the HHogGNPs have concentration in the range 10^{-7}M-10^{-10}M as we increase the NaCl concentration during synthesis. We have used Rhodamine6G (Rh6g) as the Raman tag for SERS experiments. Precisely, 20µL of each of these centrifuged samples was mixed with 180µL of 10^{-5}M aqueous solution of Rh6G in a 1.5mL centrifuge-tube-cap and the

mixture was scanned for 10s integration time. Experiments were repeated at least 5-6 times for each measurement and the average values have been reported in this manuscript.

1.7 Dynamic light scattering (DLS) measurement

To determine the surface charge and to monitor its values with varying amounts of NaCl we measured zeta potential of HHogGNPs by using a ZetaSizer Nano-ZS dynamic light scattering (DLS) device (Malvern Instruments). The synthesized HHogGNPs showed a negative zeta potential (-34 mV to -15 mV) depending on the amount of NaCl (final Cl^- concentration in the mother solution varies between 250μM-40.25mM) added during the synthesis. The value of zeta potential reduces gradually with the increment of NaCl concentration, and vice versa.

1.8 MTT Assay Study:

For dark-toxicity study we have selected RAW 264.7 mouse macrophage cell lines. We have tested the dark-toxicity for four different sets (1.7mM, 3.4mM, 10.2mM, and 17mM NaCl-induced HHogGNPs) along with the control (without nanomaterials). For each NaCl-induced HHogGNPs we made two samples for each set, one without centrifugation and another one after centrifugation to avoid excess reagent. RAW 264.7 cells were plated onto a 96-well plate (2×10^4 cells in 180μL of DMEM culture medium supplemented with 10% heat inactivated FBS, 2mM L-glutamine, 10mM HEPES and 1mM sodium pyruvate). After 24h of incubation at 37^0C in 5% CO_2 environment, 20μL of the each NPs were added to each well. Plates were again incubated at 37^0C in 5% CO_2 environment for an additional 24h. After the incubation, MTT solution was added to each well and incubated for another four hours maintaining the same conditions. The cells were washed twice with 1X PBS and the formazan crystals were dissolved with MTT dissolving solutions (11g SDS in 50mL 0.02M HCl mixed with 50mL isopropanol). The plate was incubated for 20min in room temperature and absorbance was recorded at 570nm. For each set we have performed three independent experiments keeping all the parameters same. The cell viability (% survival) was calculated as % related to the untreated control cells.

2. Results

2.1 The control experiment with ascorbic acid only

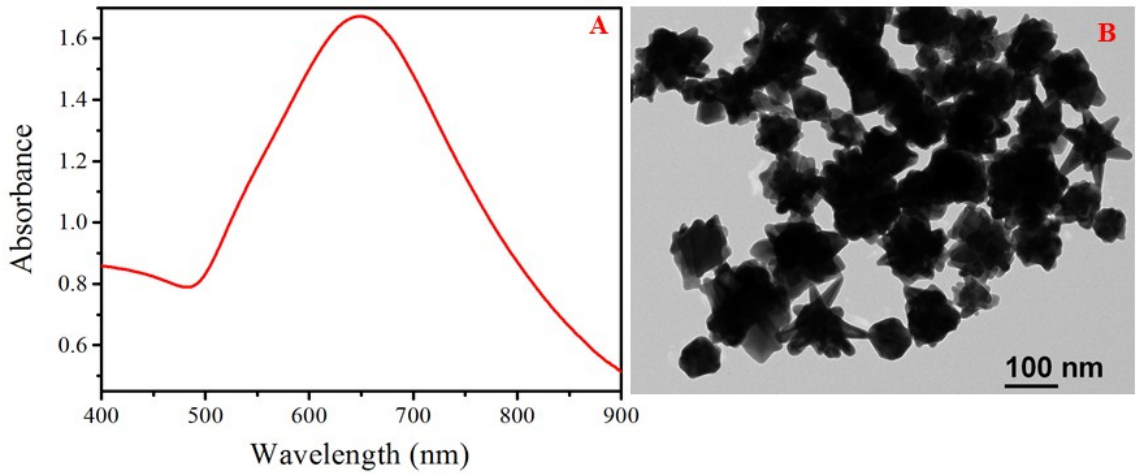

Figure S1: (A) Absorption spectra of gold nanostars synthesized by reducing Au(III) with ascorbic acid only (in the absence of TSC, $AgNO_3$ and NaCl) as a control, and (B) corresponding TEM image of the obtained gold nanostars.

2.2 Large area TEM and SEM image

Recording of large area TEM and SEM is important to find out their monodispersity nature and to evaluate their aggregation behaviour. **Figure S2** represents the corresponding large area TEM and SEM recorded from 10mM NaCl-based HHogGNPs.

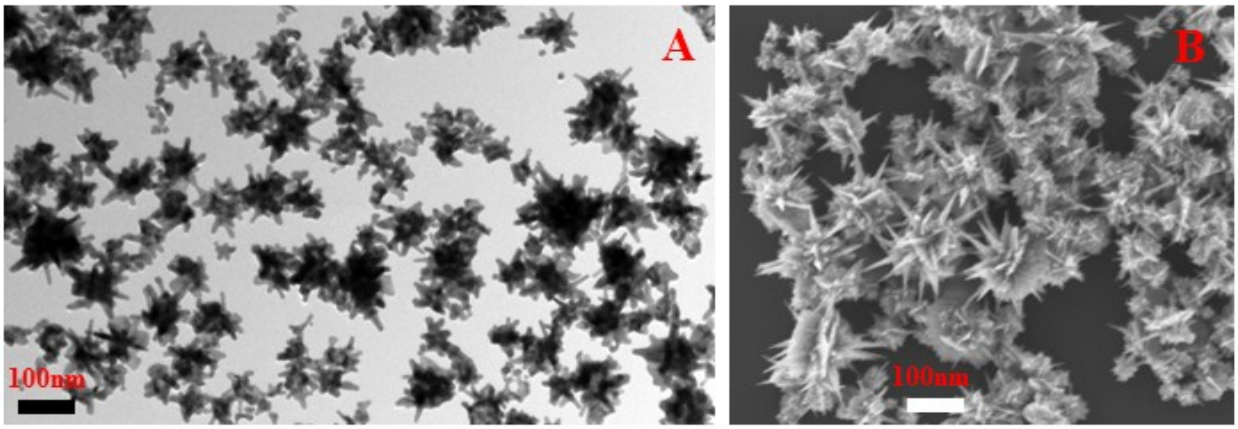

Figure S2: (A) Large area TEM and (B) SEM image of HHogGNPs synthesized by using 10mM NaCl in the mother solution.

2.3 DDSCAT Theoretical method

DDSCAT Theoretical method has been implemented for the simulation of extinction coefficient, Surface Plasmon Resonance and absorption spectra as a function of the tip-to-tip distance of HHogGNPs. The calculated extinction constant factor ($Q_{\_ext}$), Scattering constant factor ($Q_{\_\mathrm{sca}}$) and absorption constant factor ($Q_{\_\mathrm{abs}}$) are listed in **Table S1** to quantify extinction coefficient (ε in $M^{-1}cm^{-1}$).

The variation of molar extinction coefficient (ε) with the volume and SPR maxima (in μm) with the tip-to-tip distance of HHogGNPs is calculated for different sized simulated particles as shown in **Figure S3**. Our calculated SPR maxima and extinction coefficients show that the values increase with particle size. Similarly, the effect of scattering is also observable as we increase the particle size. Furthermore, our results show that surface plasmon resonance (SPR) depends on the size/area of the nanoparticle.

Table S1: The calculated geometrical properties (Tip-to-tip distance, volume, and surface area), SPR maxima, absorption constant factor ($Q_{\_\mathrm{abs}}$), scattering constant factor ($Q_{\_\mathrm{sca}}$) and extinction coefficient (ε) for modelled HHog nanoparticles.

Tip-to-tip distance (nm)	Volume ($\times 10^3$ nm^3)	Surface ($\times 10^3$ nm^2)	SPR maxima (μm)	Q_{abs}	Q_{sca}	ε $(M^{-1}cm^{-1})$
9 ± 1	0.0027	0.037	0.548	0.551	0.000	3.37×10^9
15 ± 1	0.0222	0.150	0.597	0.904	0.002	22.63×10^9
23 ± 2	0.0750	0.339	0.658	1.180	0.010	6.69×10^{10}
35 ± 3	0.2534	0.762	0.731	2.025	0.035	2.60×10^{11}
55 ± 3	0.9136	1.793	0.852	3.360	0.161	1.04×10^{12}
85 ± 3	3.0834	4.035	0.960	5.108	0.703	3.89×10^{12}

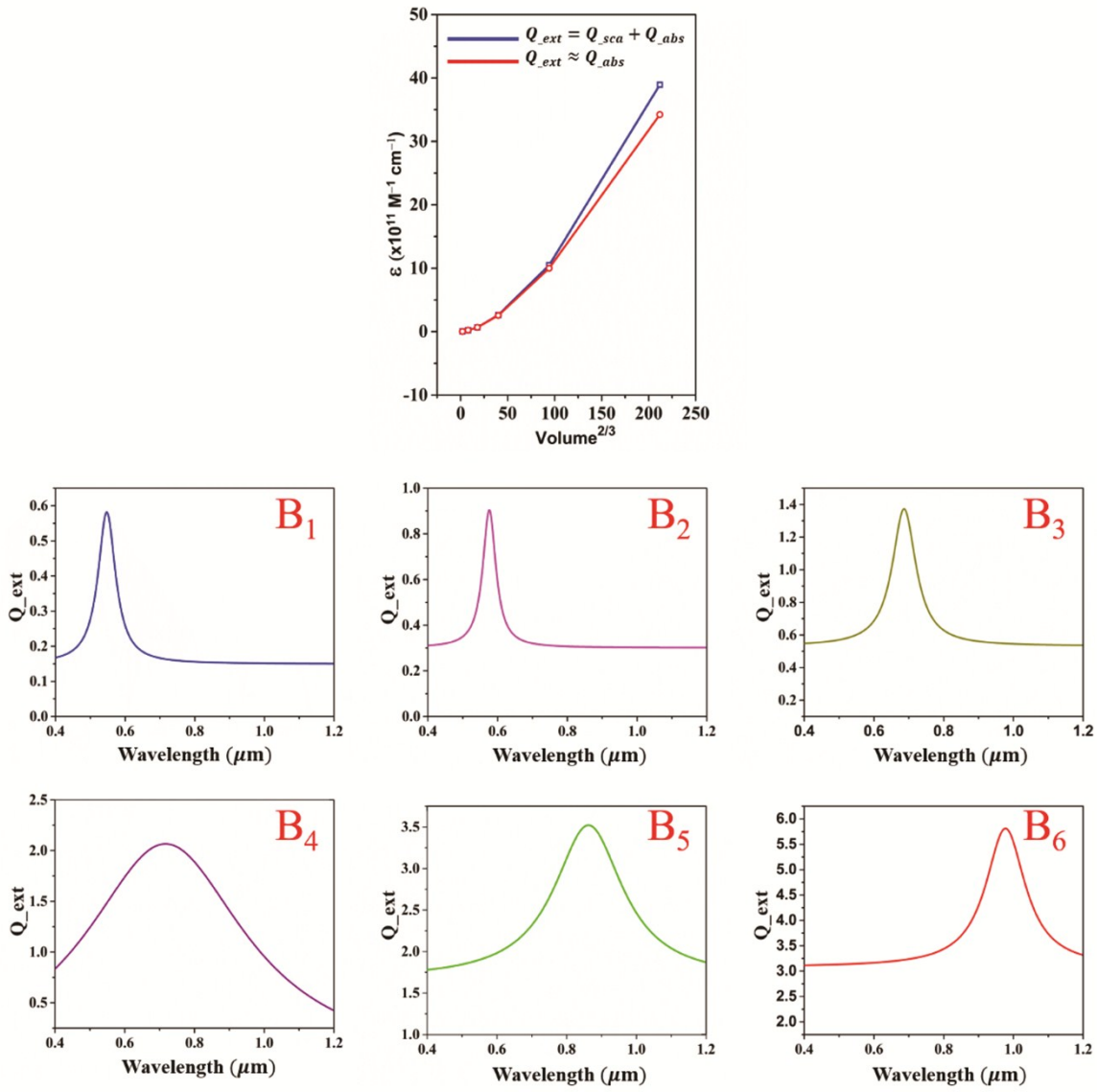

Figure S3: (A) Variation of molar extinction coefficient (ε) with the volume of the HHog nanoparticles and SPR maxima (in μm) for different tip-to-tip distances (B_1: 9 ± 1nm, B_2: 15± 1nm, B_3: 23±2nm, B_4: 35±3nm, B_5: 55±3nm, B_6: 85±3nm,) nanoparticles.

2.4 High Resolution TEM

As SAED aperture is too big compared to the tip size it is a natural practice to take HRTEM images and then Fast Fourier Transform (FFT) to get reciprocal space information. We have taken about 30 such images and to check that entire sharp tips projecting out of the central

spherical core are oriented in {111} direction. It was not possible to check on a single structure as different tips have different zone axis. For this reason we have taken several structures and checked one or two tips. **Figure S4** represents the details of HRTEM data of three such different nanostructures.

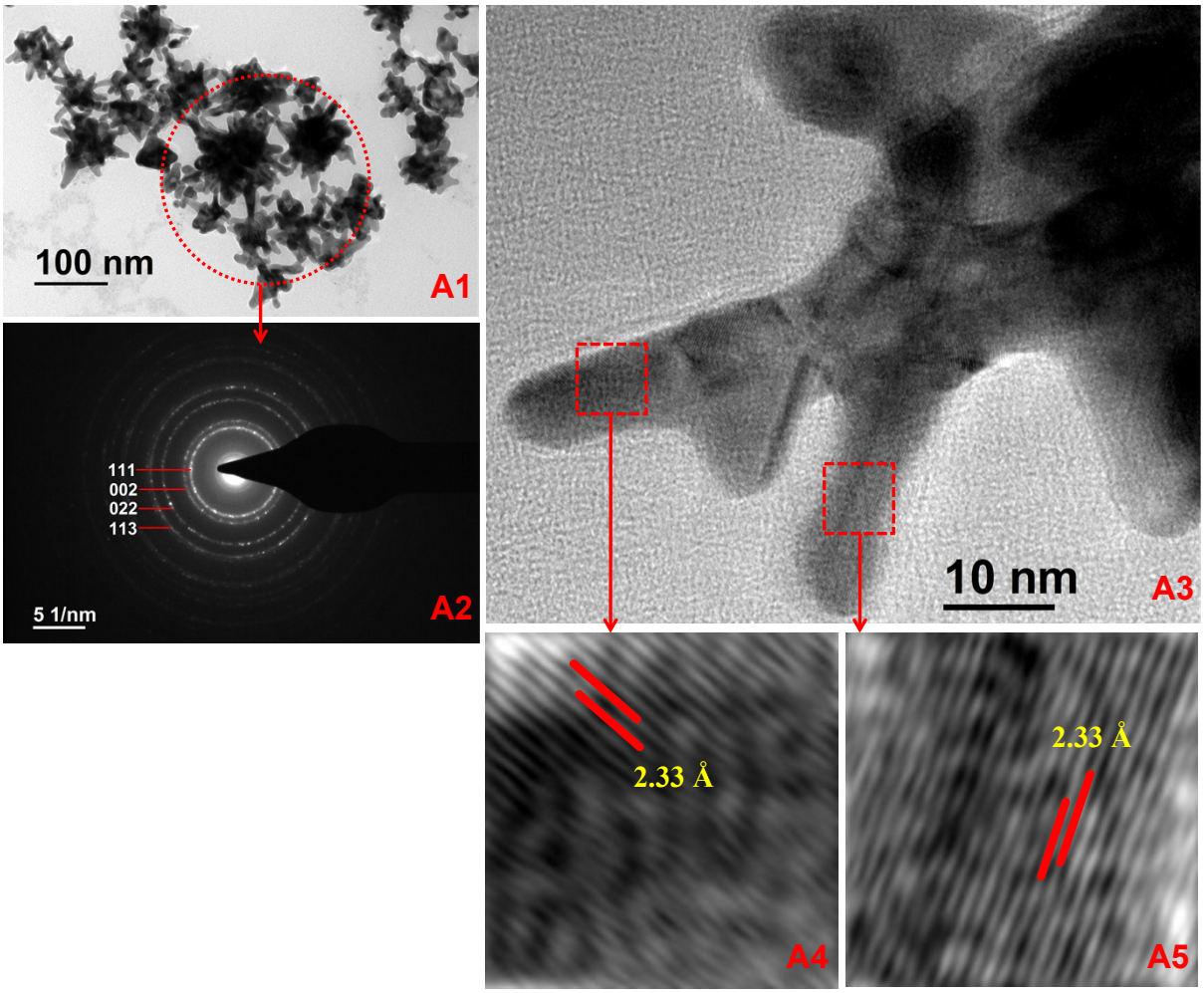

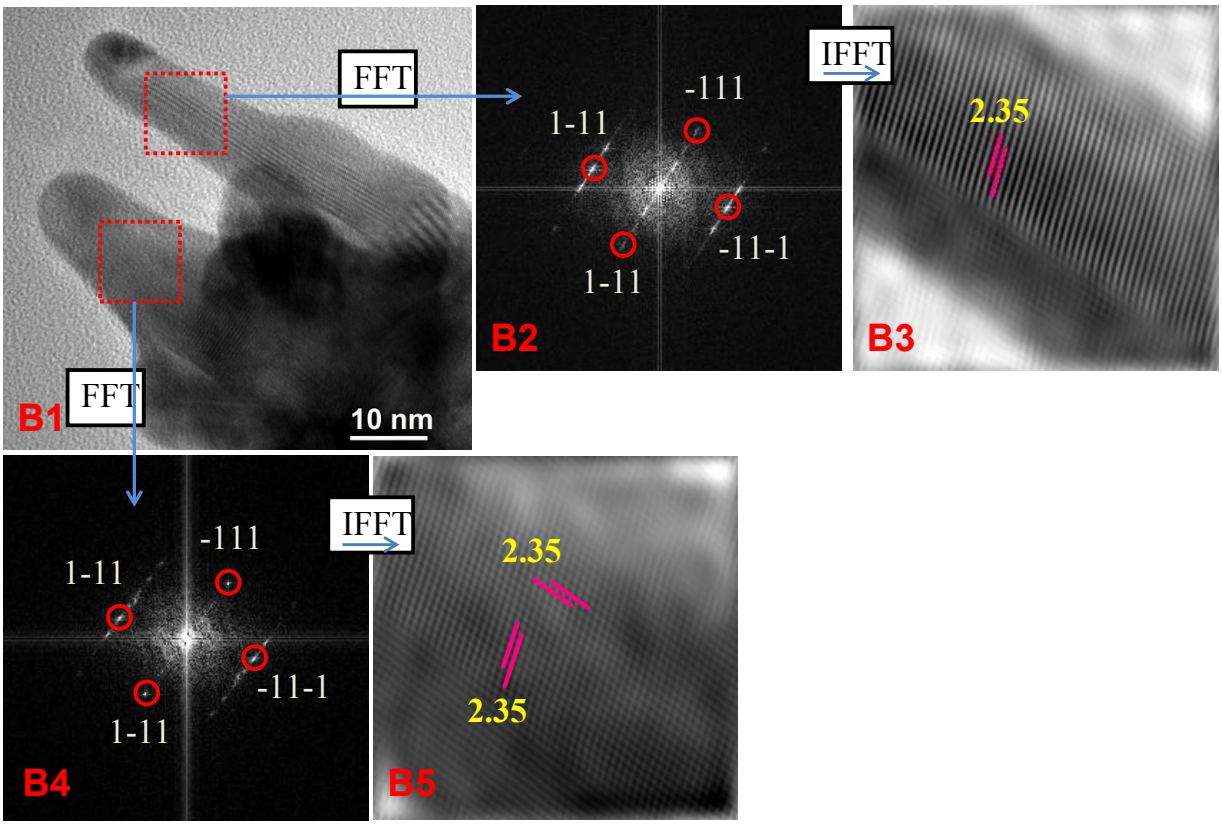
FFT
IFFT
FFT
IFFT
B1
B2
B3
B4
B5
10 nm
-111
1-11
-11-1
1-11
2.35
2.35
-111
1-11
-11-1
1-11

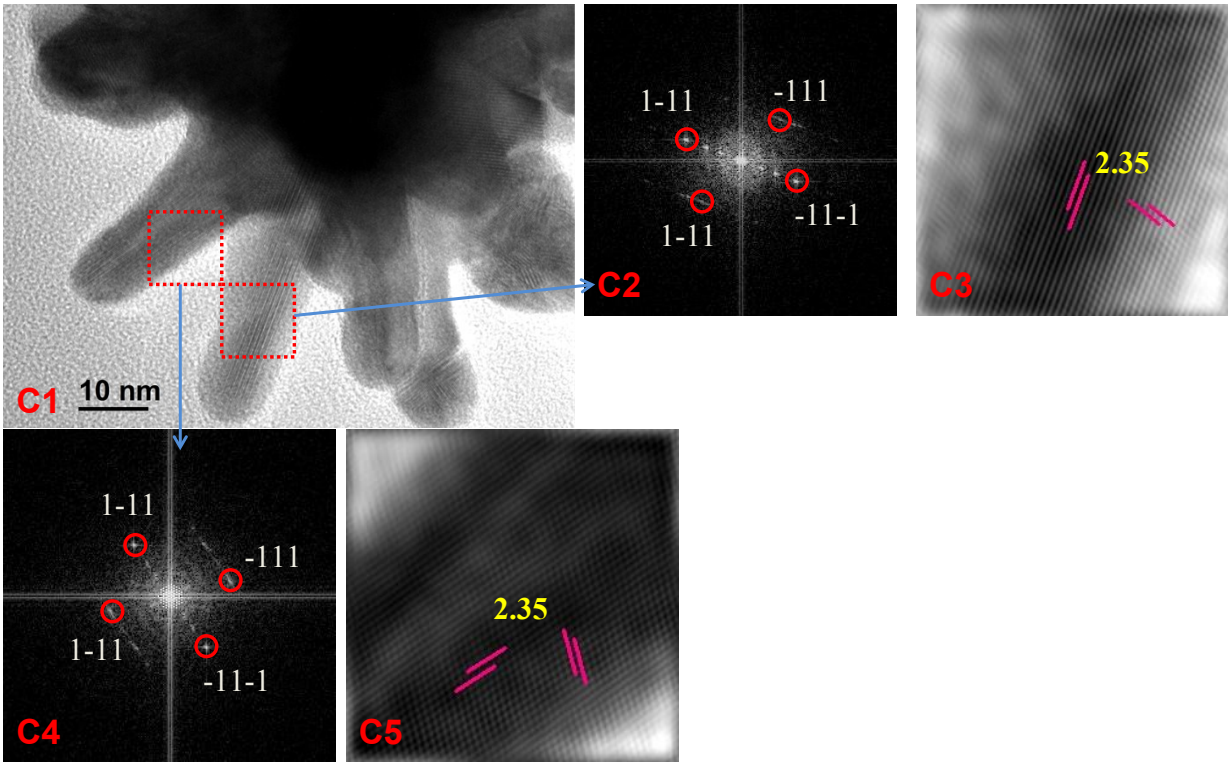
C1
C2
C3
C4
C5
10 nm
1-11
-111
-11-1
1-11
2.35
1-11
-111
1-11
-11-1

Figure S4: HRTEM of the seed-free, template-free salt-induced HHogGNPs synthesized in presence of 3.4mM NaCl. (A_1-A_5), (B_1-B_5), (C_1-C_5) represent data for three different HHog gold nanostructures.

2.5 MTT Assay

Table S2: Different samples used for the MTT-based dark toxicity test with variable NaCl concentrations and the average cell viability results for RAW 264.7 mouse macrophage cell lines.

Dose	Type of Nanomaterial	Concentration of NaCl in the HHogGNPs	% Survival	Standard Deviation
Control	Without Nanomaterials	Without Nanomaterials	100.0	0
1A	Mother Solution	1.7mM	89.8	4.1
1B	Centrifuged	1.7mM	110.9	6.8
2A	Mother Solution	3.4mM	88.6	6.9
2B	Centrifuged	3.4mM	120.8	8.2
3A	Mother Solution	10.2mM	89.4	8.6
3B	Centrifuged	10.2mM	101.7	4.7
4A	Mother Solution	17mM	100.0	1.7

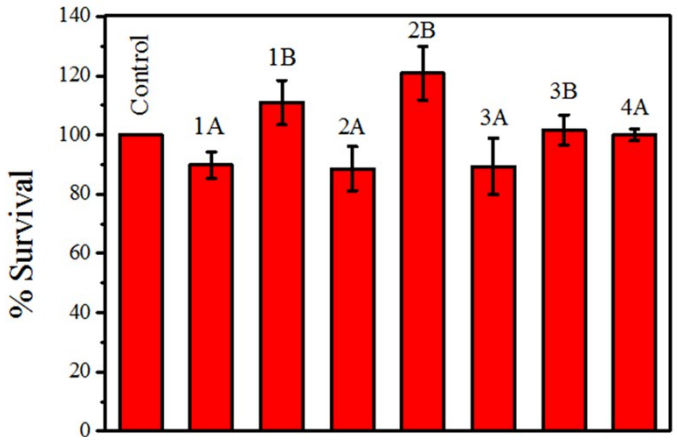

Figure S5: A comparative study (n=3) among the obtained cell viability results for samples mentioned in Table S2 applied on RAW 264.7 mouse macrophage cell lines.

2.6 Counting Number of Tips

We have taken 30 different TEM images for each hedgehog structures synthesized at a particular NaCl concentration and then counted the total number of visible spikes for 2π solid angle to get an idea about the possible number of spikes for 4π solid angle (3D-space). In the **Figure S6** the tips are marked based on which we have counted the number of tips and the average number of tips have been listed in **Table 1** in main manuscript.

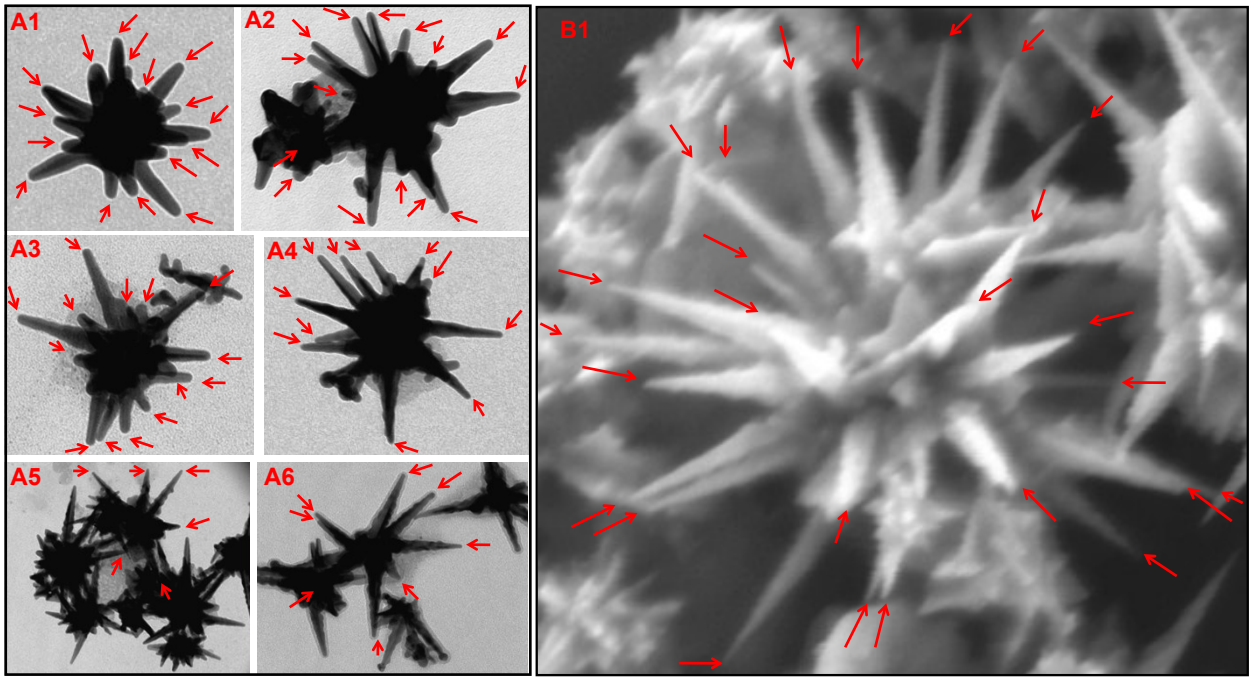

Figure S6: (A_1-A_6) are TEM images of HHogGNPs synthesized at different NaCl concentration: A_1 – 170µM, A_2 – 340µM, A_3 – 1.7mM, A_4 – 3.4mM, A_5 – 10mM, A_6 - 20mM and B1 is the SEM image of a HHogGNP synthesized in presence of 10mM NaCl.

2.7 Structural Statistics of HHogGNPs

Table S3: Detailed structural statistics of Le Chatelier's Principle based common Cl^- induced synthesized HHogGNPs

NaCl concentration (M)	170×10^{-6}	340×10^{-6}	170×10^{-5}	340×10^{-5}	10×10^{-3}	20×10^{-3}
Average particle diameter (nm), $2R_0$	220±19	220±16	220±09	220±21	220±11	220±13
Average surface-tip length (nm), h_c	60±11	69±15	80±09	89±09	93±11	95±06
Average core diameter (nm), $2R$	100±17	94±17	73±05	68±11	50±07	30±04
Average number of tips, N	32±06	28±07	26±05	20±03	16±04	10±03
Average diameter at the tip (nm), $2r^{'}$	5.0±0.9	3.6±1.1	3.2±0.6	2.6±0.7	2.4±0.2	2.0±1.0
Curvature at the tip (cm^{-1}), $\kappa = \left(r^{'}\right)^{-1}$	(4.2±0.7)× 10^6	(6.1±1.9)× 10^6	(6.5±1.2)× 10^6	(8.3±2.2)× 10^6	(8.4±0.7)× 10^6	(1.3±0.7)× 10^7
Tip base diameter (nm), $2r_c$	10±1.3	9±0.8	8±0.8	7.5±0.5	5.6±0.6	5±0.2
2D projected angle covered by the tip (degree)	12.8±1.3	10.3±1.8	7.6±0.4	7.1±0.7	5.6±0.3	4.7±0.1
Average Aspect Ratio (AAR) of surface tips	9±3.0	14.4±4.6	17.5±7.5	23.1±11.2	27.7±11.1	33.3±13.7
Zeta potential (mV)	-32	-29	-22	-20	-17	-16
RSA	1.04±0.1	1.05±0.2	1.74±0.6	1.5±0.2	1.75±0.5	2.8±0.7